

1993 3.25
492441

545-76

TUNNELING MAGNETIC FORCE MICROSCOPY

N 93-22194

P. 10

Dr. Edward R. Burke
Laboratory For Physical Sciences
8040 Greenmead Dr.
College Park, MD 20740

Dr. Romel D. Gomez, Dr. Amr A. Adly, Dr. Isaak D. Mayergoyz
Department of Electrical Engineering, Institute for Advanced Computer Studies
University of Maryland
College Park, MD 20742

ABSTRACT

We have developed a powerful new tool for studying the magnetic patterns on magnetic recording media. This was accomplished by modifying a conventional scanning tunneling microscope. The fine-wire probe that is used to image surface topography was replaced with a flexible magnetic probe. Images obtained with these probes reveal both the surface topography and the magnetic structure. We have made a thorough theoretical analysis of the interaction between the probe and the magnetic fields emanating from a typical recorded surface. Quantitative data about the constituent magnetic fields can then be obtained. We have employed these techniques in studies of two of the most important issues of magnetic recording: data overwrite and maximizing data-density. These studies have shown: (i) Overwritten data can be retrieved under certain conditions, and (ii) Improvements in data-density will require new magnetic materials. In the course of these studies we have developed new techniques to analyze the magnetic fields of recorded media. These studies are both theoretical and experimental and combined with the use of our magnetic force scanning tunneling microscope should lead to further breakthroughs in the field of magnetic recording.

INTRODUCTION

This paper updates and summarizes the work that we have performed [refs. 1-7] in developing a magnetic force scanning tunneling microscope. We have developed this device as a tool to study important questions in the rapidly evolving field of magnetic recording. Two of the questions that we have addressed are: (1) What happens when data on magnetic media is overwritten with new data? and; (2) What are the limits of data-density (the amount of data that can be recorded in a given area) in magnetic recording? Ideally, one might hope that the answer to the first question is: When old data is overwritten with new data, the old data is completely erased and only the new data is present. If the real world is less than the ideal, then new questions are posed: Under what conditions can the old data be retrieved? How much can be retrieved? Do different types of data respond differently? What can one do to insure complete erasure? Is the new data corrupted in any way by the overwrite process? In our studies we have tried to address all of these questions. The most important discovery of our work is that under certain conditions *all* of the overwritten data can be retrieved.

For the question of data density, we have demonstrated that there are limits to the density that can be obtained with present day materials. This then leads to the question: What are the important parameters that can be changed to increase the data density? This is the most important question in magnetic recording technology and it has been discussed extensively in the literature. What we have demonstrated with our studies is how the magnetic force scanning tunneling microscope can be used to study the processes that limit the data density and how the new theoretical studies that we have developed will lead to an improved understanding of these processes.

TECHNIQUE

Rice and Moreland [8] have shown that magnetic data on a hard disk can be imaged with a tunneling microscope by using a flexible triangular probe cut from a thin film of magnetic material. We have assembled a similar device [1]. This technique is a straightforward and useful extension of scanning tunneling microscopy (STM) [9]. In this new technique, a flexible magnetic probe is used in place of the fine metallic tip employed in STM for imaging of surface topography. The magnetic probe is deflected as it interacts with the local magnetic fields. The deflections change the tunneling gap (the probe-sample separation), which correspondingly change the tunneling current. A feedback system continuously adjusts the vertical displacement of the probe to keep the current constant as it is rastered across the surface. The changes in the vertical displacement are measured and recorded 400 times on a single scan. The image is constructed from 400 rastered scans. Thus, as schematically shown in Fig. 1(a), the

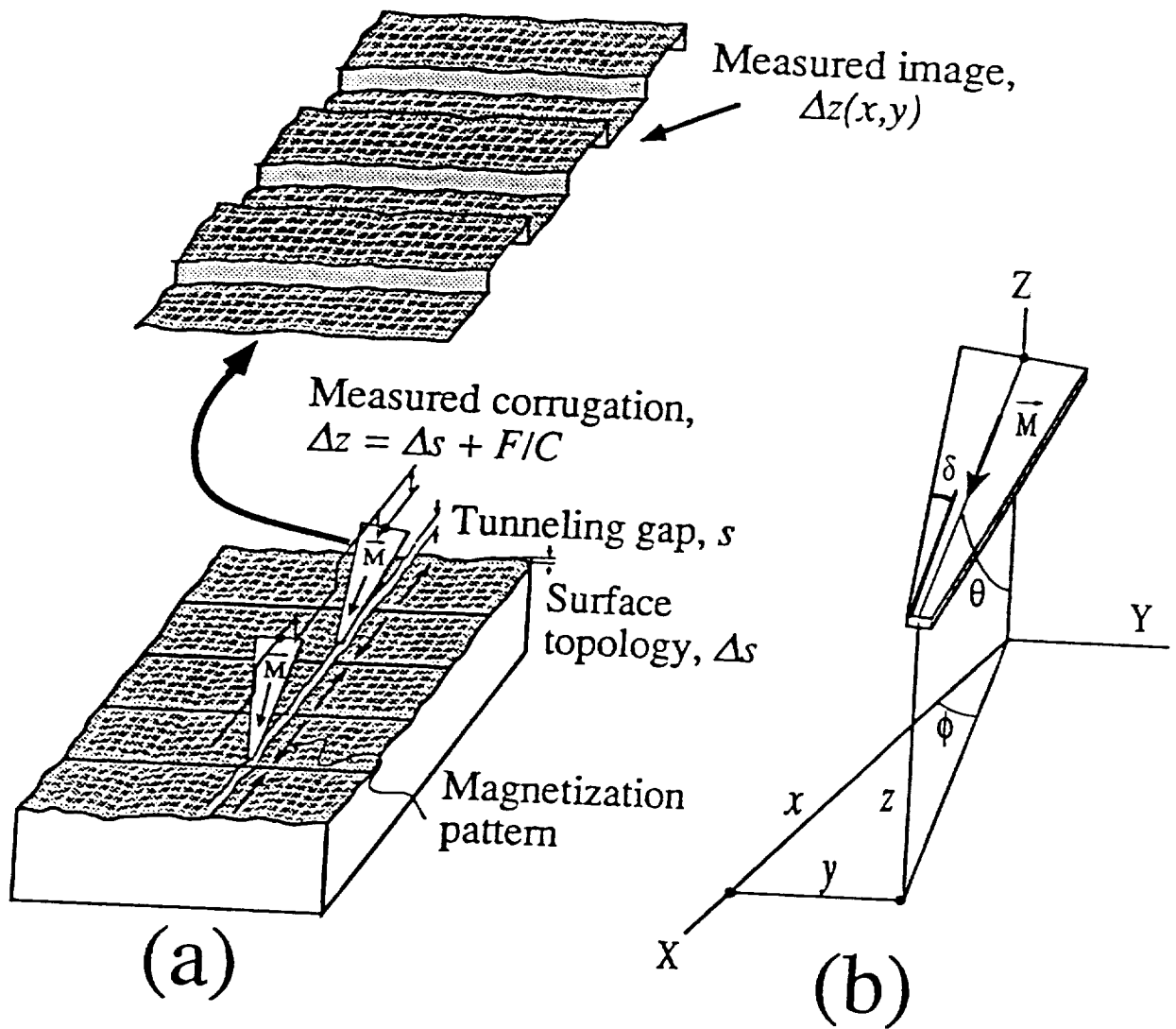


FIG. 1. (a) Schematic diagram of magnetic force scanning tunneling microscopy. The deflection of the probe due to its interaction with the local surface magnetic fields is mapped as a function of its lateral position (see text) and (b) probe geometry used in the analysis.

resulting image of vertical displacements represents the local magnetic field variations combined with the surface topography variations. The vertical displacements, and the in-plane rastering position are all controlled and measured by accurate piezoelectric elements.

A typical image is shown in Fig. 2. The image shows magnetically recorded data on a commercial hard disk. Three distinct data tracts are visible here, each having a width of approximately 45μ . The tracks are separated by about 12μ of non magnetized region. Magnetized regions appear as broad ($\sim 6 \mu$) depressions bounded by relatively narrow ($\sim 2 \mu$) bright protrusions. The "height" of these magnetized regions are of the order of 150-200 nm, which is roughly a factor of 10 larger than the surface roughness. The surface roughness shows up as the fine lines running perpendicular to the magnetic data. These fine lines are caused by the final machining of the aluminum disks. The disks appear mirror-smooth to the naked eye and the fine lines, which are readily apparent here, can only be observed with the most sophisticated optical microscopes. In Fig. 2(b), we show a high-resolution magnification roughly corresponding to the upper right-hand corner of the image. Two different types of tracks are clearly visible, distinguished by the change in relative sizes of depressions and protrusions; which demonstrates the ability of our device to distinguish between different directions of surface magnetization. The 3D image shown in Fig. 2(b) was constructed through system software. The variations in the amplitude of the displacements can be seen along the lower edge of the image in Fig. 2(b). To obtain quantitative information about the magnetic fields emanating from the surface, one would have to know how the displacement amplitude is related to the magnetic fields. In order to obtain this information, we have made a complete theoretical analysis [2] of the interaction between a flexible triangular probe and a typical magnetic pattern on a recorded surface. The use of this analysis allows the measurement of the magnetic fields of the recorded patterns imaged by a magnetic force scanning tunneling microscope.

THEORY

Magnetic Fields

Fig. 1(b) shows the geometry for our calculations. We assume that the recorded signal is a repetitive, symmetric pattern of wavelength λ in the x direction, with infinite extent in the y direction. The magnetic field H from the pattern can be expressed as the gradient of a scalar potential Φ ,

$$H = -\nabla\Phi \tag{1}$$

The scalar potential will be the solution of Laplace's equation and can be written as,

$$\Phi(x,z) = \sum_{n=1}^{\infty} \Phi_n e^{-kz} \cos kx, \tag{2}$$

where $k = 2\pi n/\lambda$, and the coefficients Φ_n match the series solution to the particular field pattern. The field pattern will of course depend on the magnetization distribution within the recorded media. We have found it convenient to express the magnetization in Fourier series. If we assume that the recording media is so thin that the magnetization is uniform through the thickness of the film, then there are two different magnetization patterns that will lead to the scalar potential given by (2). The first pattern is a magnetization in the plane of the film given by,

$$M_x = M_s \sum_{n=1}^{\infty} m_{x,n} \sin kx, \tag{3}$$

where M_s is the saturation magnetization and the $m_{x,n}$ are the normalized Fourier coefficients. The other magnetization pattern that would lead to the scalar potential (2) is a magnetization perpendicular to the plane of the film given by,

$$M_z = -M_s \sum_{n=1}^{\infty} m_{z,n} \cos kx, \tag{4}$$

where the minus sign is a mathematical convenience. The fields can be constructed from linear combinations of (3) and (4), and if we use Maxwell's equations and make the transverse component of H and the normal component of B

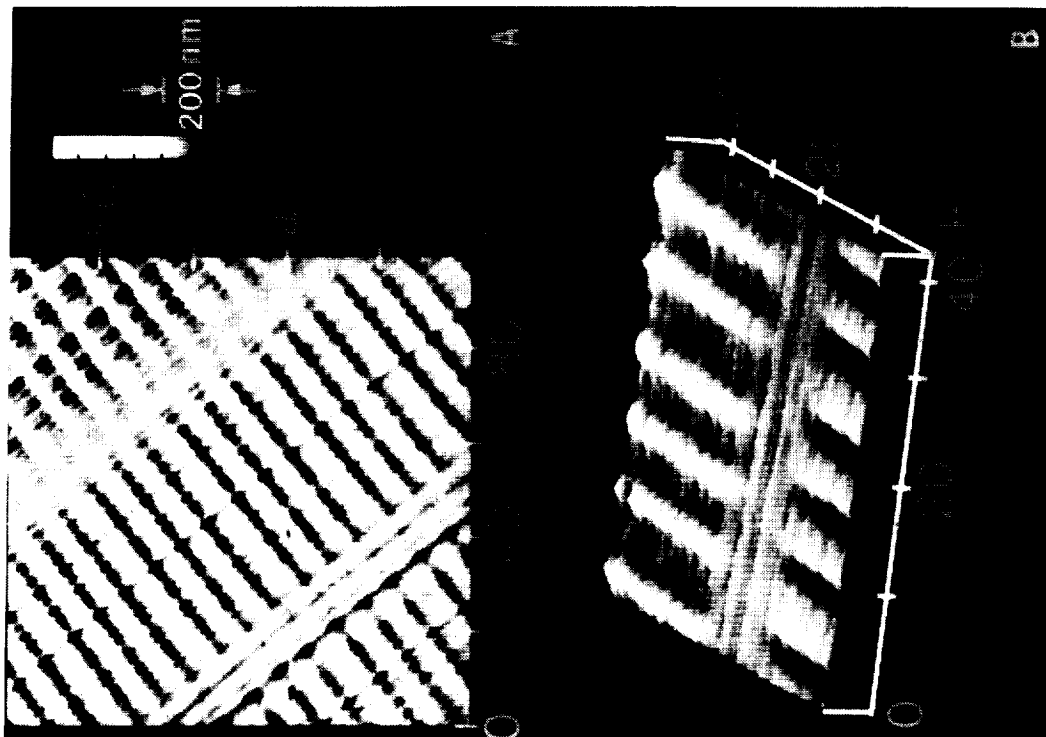


FIG. 2. (a) A large field-of-view MFSTM image showing the recording tracks of a computer hard drive magnetic media, and (b) perspective surface plot of a magnified view of the upper right-hand corner showing two different track types, distinguished by the lengths of the protrusions and depressions.

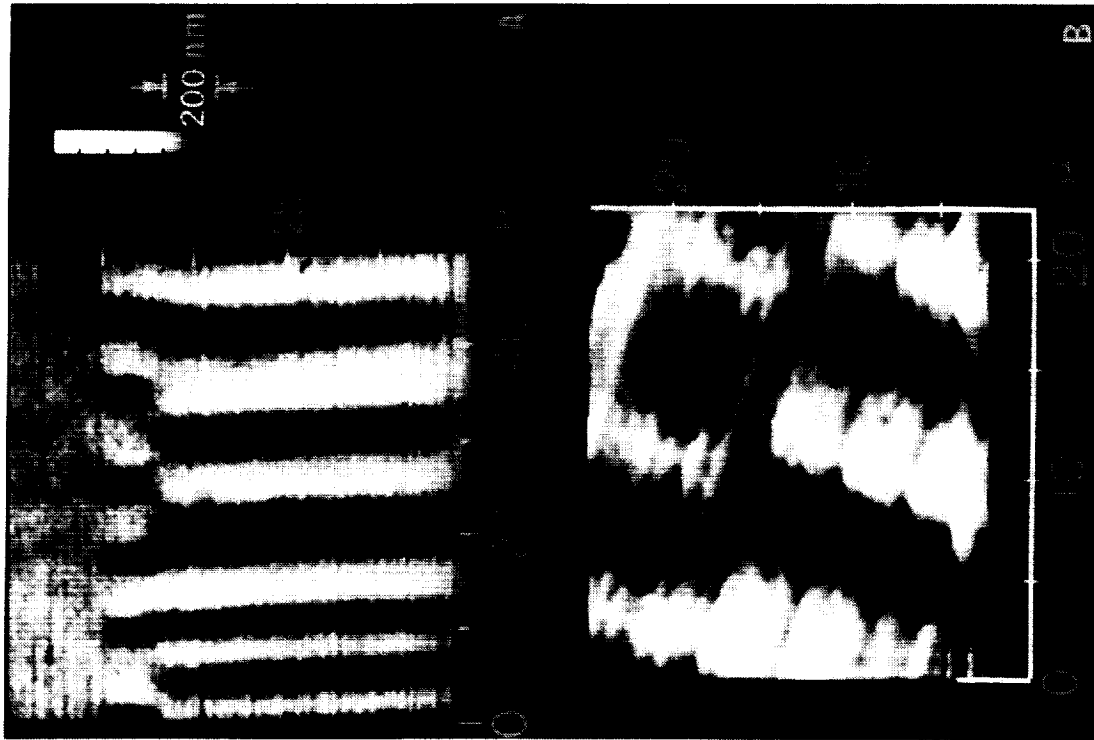


Fig. 3. Overwritten data on conventional commercial rigid disk showing: (a) remnant of previous data, and (b) erase band.

($\mathbf{B}=\mathbf{H}+4\pi\mathbf{M}$) continuous at the media surface, then we can solve for the coefficients Φ_n . We will leave the details of these calculations to a later paper. For now we will simply give the result which is,

$$\Phi_n = -2\pi M_s(1 - e^{-kd})(m_{x,n} + m_{z,n}) / k, \quad (5)$$

where d is the thickness of the recording media. We have used (5) to construct numerous field distributions, including all the ones we could find in the literature [10], [11], [12]. The point is that we can use these techniques to find the magnetic fields from virtually any distribution of magnetization. We now return to the major problem at hand: the interaction between these fields and the probe tip.

Energy of Interaction

The Energy of interaction between the field from the pattern and the last domain on the probe tip can be expressed as [10]

$$E = -\int H \cdot M \, dV, \quad (6)$$

where M is the magnetization of the last domain on the probe tip, and V is the volume of the domain. To perform the integral of (6) we make the following assumptions: (i) the domain is magnetized along the probe axis by shape anisotropy, (ii) the domain is much longer than λ so that the limit of integration in the z direction can be extended to infinity, and (iii) the thickness of the probe, t , is much less than the wavelength λ . Rugar et al. [12] have shown that the last domain on their probe tip was about 20μ in length, and since most patterns on modern recording surfaces have a wavelength smaller than this, assumption (ii) is not unreasonable. The thickness of the probe is much less than a micron which is about the smallest wavelength currently available. Using these assumptions, the integral (6) was evaluated in [2] with the result,

$$E = Mtw \sum_{n=1}^{\infty} \Phi_n e^{-kz} \left\{ \cos kx \frac{\sin((kw \sin \phi) / 2)}{(kw \sin \phi) / 2} + \frac{\tan \delta}{wk} [A_+ \cos k(x - x_+) + A_- \cos k(x - x_-)] \right\}, \quad (7)$$

where,

$$A_{\pm} = 1 / \sqrt{\cos^2 \theta + (\sin \theta \cos \phi \pm \tan \delta \sin \phi)^2}, \quad (8)$$

and,

$$x_{\pm} = \pm \frac{w}{2} \sin \phi + \frac{1}{k} \tan^{-1} \left(\frac{\sin \theta \cos \phi \pm \tan \delta \sin \phi}{\cos \theta} \right). \quad (9)$$

The integrals were performed so that the point (x,z) is the coordinate of the probe tip. The first term in (7) is due to a magnetic charge Mtw at the tip of the probe. The magnetic potential is weighted by a sampling factor caused by the variation in the field across the width w of the probe tip. The next two terms can be thought of as the contributions from the magnetic charges on the sides of the probe, separated from the tip by the distances x_{\pm} . The equations (7-9) give a complete expression for the energy of interaction between the probe and the fields from the recorded media.

Probe-Tip Displacement

The quantity that is measured by the tunneling microscope is the displacement Δz of the probe tip. The displacement is caused by both the surface topography and the magnetic interaction between the probe and the magnetic field from the surface pattern. If the probe tip is properly designed, the interaction will predominate and the surface roughness will appear as a background noise.

If the probe is constrained to rotate in the θ direction, the displacement will be given by $l \sin \theta \Delta \theta$, where l is the length of the probe's moment-arm. A force F_N normal to the probe's tip will cause a rotation in the θ direction such that $lF_N = -K\Delta \theta$ where K is the tip torque constant. The displacement Δz is then given by

$$\Delta z = -\frac{l^2 F_N \sin \theta}{K} \quad (10)$$

The force acting on the tip is the gradient of the energy $F = -\nabla E$ so that (10) becomes

$$\Delta z = \frac{l^2}{K} \left(\cos \theta \cos \phi \frac{\partial E}{\partial x} + \sin \theta \frac{\partial E}{\partial z} \right) \sin \theta. \quad (11)$$

Using (7), (11) becomes, after some manipulation,

$$\Delta z = -\frac{l^2 M t w \sin \theta}{K} \sqrt{\cos^2 \theta \cos^2 \phi + \sin^2 \theta} \sum_{n=1}^{\infty} \Phi_n k C e^{-kz} \sin \left(kx - \beta + \tan^{-1} \frac{\sin \theta}{\cos \theta \cos \phi} \right), \quad (12)$$

where,

$$C = \sqrt{\left[\frac{\sin((kw \sin \phi) / 2)}{(kw \sin \phi) / 2} + \frac{\tan \delta}{kw} (A_+ \cos kx_+ + A_- \cos kx_-) \right]^2 + \left[\frac{\tan \delta}{kw} (A_+ \sin kx_+ + A_- \sin kx_-) \right]^2}, \quad (13)$$

and,

$$\beta = \tan^{-1} \frac{\tan \delta (A_+ \sin kx_+ + A_- \sin kx_-)}{\frac{\sin((kw \sin \phi) / 2)}{(\sin \phi) / 2} + \tan \delta (A_+ \cos kx_+ + A_- \cos kx_-)}. \quad (14)$$

Equations (12)-(14) give a complete description of the interaction between the probe and the recorded pattern. In general, the equations are quite complicated and their usefulness is not readily apparent. In the case when the probe lines up with the pattern ($\phi = 0$) the equations reduce to a simple form,

$$\Delta z = -\frac{l^2 M t w \sin \theta}{K} \left[H_x \cos \theta + H_z \sin \theta + 2 \frac{\tan \delta}{w} \int_0^x H_x dx' \right]. \quad (15)$$

The first two terms give the interaction between the magnetic field and the magnetic charge at the tip. The next term gives the effect of the charges on the sides of the probe. This last term was written in the integral form so that it could be expressed in terms of the magnetic field H_x . It could have been written in terms of H_z in which case it would have been identical to the expression for the flux picked up by a conventional recording head. Equation (15) is an important result because it shows that, if the third term can be made small, then the images can be related to the magnetic fields at a point. We call this "the point charge model" and we have expanded on it in [6] and [7].

Equation (15) can be used to obtain relative values of the magnetic field components H_x and H_z . To obtain absolute values, the probe would have to be calibrated in a known field to obtain the factor $l^2 M t w / K$. One way to obtain the fields from (15) is to obtain three images at three different values of the angle θ . The fields H_x and H_z can then be obtained at every point from a linear combination of the three images. For example, if three images, $\Delta z(\theta)$, were obtained at the angles of 30, 45, and 60 degrees, then H_x and H_z could be solved for, to obtain,

$$H_x = \frac{K}{l^2 M t w} [18.02 \Delta z(30^\circ) - 29.35 \Delta z(45^\circ) + 13.56 \Delta z(60^\circ)], \quad (16)$$

$$H_z = \frac{K}{l^2 M t w} [23.48 \Delta z(30^\circ) - 29.35 \Delta z(45^\circ) + 10.40 \Delta z(60^\circ)]. \quad (17)$$

Since all the data used to construct the images is available in digital form, it is a simple matter to combine the images using (16)-(17) to obtain the magnetic fields. The main experimental difficulty with this procedure would be in obtaining the images at exactly the same location every time. One way to alleviate this problem would be to use the topological features of the surface as guide-points. We have thus made a complete theoretical analysis of how the magnetic force scanning tunneling microscope can be used to obtain the magnetic fields from recorded media as a function of all of the relevant parameters.

DATA OVERWRITE

Overwrite performance is a major concern in magnetic recording since data detection can be corrupted by previously recorded patterns when sufficient overwrite is not achieved. Even with direct overwrite, portions of previously recorded data can persist and be detectable. Tracking misregistration, or slight deviations in positioning of the recording head from the original track, could leave even more significant portions of previous data along the track edge [3]. Fig. 3(a) shows a $50\mu\times 50\mu$ image of a commercial rigid disk with overwritten data. The new data appears as the long alternating bright protrusions and dark depressions representing oppositely magnetized regions along the track. Remnants of the previously recorded data appear as localized regions extending by a few microns from the upper track edge. It should be emphasized that this pattern was not deliberately constructed but was found on a previously used disk. The overwritten data can be completely recovered by simply reading it off on a bit-by-bit basis.

The high resolution image of a different overwritten region in fig. 3(b) suggests some interesting characteristics of the erase band. The regions where the old and new data coincide create continuous magnetization between the old and new tracks, as exhibited by the extreme left transition. This is not the case for the two succeeding transitions, however, where the new set is out-of-phase with the old set. Here, the old data are truncated prior to the emergence of the new data, leaving about a micron wide gap with no definite magnetization. This behavior is consistent with current notions of the erase band [13,14]. The write field within this narrow band was above the coercivity of the media to reduce the magnetization at those areas (which truncated the bright stripes of the old data) but the magnitude was not high enough to create new well defined magnetizations.

We have continued these investigations by obtaining images of deliberately overwritten data on thin film disk media. We have examined the relationship between the persistence of overwritten data and the radial offset of the recording head, as well as the effects of the recording density [5]. The effect of a previously recorded pattern can be detected even when distinct remnant transitions can not be identified. At recording frequencies in the range of 10 MHz, the previously recorded pattern affects the newly recorded track even at small ($>2\mu$) offsets, by introducing apparent lengthening or shortening of the track-width depending upon the relative phases of old and new patterns. Presumably, one could still extract the overwritten data in this case but it would require much more analysis. Distinct portions of overwritten data remain on the surface for offsets in excess of 2μ . At low recording frequencies in the range of 1 MHz, larger offsets ($>4\mu$) are needed to detect previously recorded data. In this case, the non-uniform magnetization introduces recorded cells of "trapezoidal" cross sectional area. This effect is less severe at high frequencies, and plays a crucial role in extending the required minimum offset.

DATA DENSITY

Despite recent advances in media processing technology and the demonstration of storage densities beyond 1 Gigabit/square inch [14], our understanding of processes that lead to reduction in signal strength as the wavelength is decreased is still under development. The process involves a complex interplay between media and recording head properties. While a great deal of theoretical and experimental work has been performed, one of the difficulties in determining the roles played by the different mechanisms is the lack of systematic experimental data to characterize magnetization patterns with sufficient spacial resolution. What we have done is to show how the magnetic force scanning tunneling microscope (MFSTM) can be used as a powerful tool to study this problem.

In this work, we are concerned with direct real space imaging of recorded patterns. We performed a series of MFSTM measurements of magnetization patterns which were written with progressively increasing densities. We then analyzed the pattern behavior as the wavelength was reduced. This work extends previously reported investigations of high density recording on longitudinal recording media by using magnetic force microscopy [13]. In contrast with those MFM measurements, the current MFSTM based technique allows a more straightforward interpretation of the images and thus facilitates quantitative analysis. Specifically, we make quantitative estimates of the transition length by comparing image profiles with calculated lineshapes based upon an arctangent model for the transitions. We then discuss possible mechanisms that play major roles in causing self-erasure at high recording densities.

Experiment

Measurements were made on a commercially available rigid disk with patterns recorded on a precision spin stand system. Fig. 4 shows a series of recorded transitions in the range of 100 to 2000 FR/mm, which correspond to recorded wavelengths λ in the range from 20 μ to 1 μ . All images were obtained using a single imaging probe so that comparisons between different tracks are independent of probe specific properties.

In addition to trackwidth reduction [16], we find significant variations in the behavior of these patterns with increasing density. In the range from 100 to 600 FR/mm ($20\mu \leq \lambda \leq 3.1\mu$), the transitions are well defined and exhibit very little zigzag across the track. This is consistent with previously reported magnetic force microscope measurements on longitudinal recorded patterns [13]. Similarly, the amplitudes of the magnetic features are more or less constant, indicating that the relative strength of the fields do not vary significantly from the longest wavelength down to about 3.1 μ . At higher densities, the amplitudes decrease sharply and the patterns gradually lose their detail. The transitions start to become fuzzy, and in certain areas, they appear to merge together. The bits coalesce to form localized patches, becoming more noticeable for $\lambda < 2.2\mu$. At 1 μ wavelength, the track edges become indistinct and the size of the coalesced regions has increased considerably, leaving individual transitions barely discernible. This effect could be associated with either poor high density performance of the media or the frequency response of the recording head. It is quite possible that recording fields perturb neighboring previously recorded bits, which reduces their magnetizations.

Discussion

We begin our analysis by deriving an estimate of the transition length. Close inspection of the images in Fig. 4 show that the lineshapes vary with the wavelength. This is illustrated clearly in Fig. 5 where a series of average line profiles from representative images in Fig. 4 are presented as solid curves. The peak occurs very near the left transition edge at the lowest recording frequency, and gradually moves to the center as the wavelength is decreased. This can be explained using a model that allows the transition length parameter to become a substantial fraction of the bit length.

As shown previously, the deflection Δz is given by (15). For the probe that we used, $\delta=15$ degrees and $w=2.5\mu$. To use (15), expressions must be found for the magnetic field caused by the recorded magnetization. For this study we will assume that the magnetization is a symmetric series of alternating polarities with arctangent transitions. The Fourier series that approximates the magnetization pattern is given by

$$M_x = 8M_s \sum_{n=\text{odd}} \frac{e^{-ka}}{k\lambda} \sin kx, \quad (18)$$

where a is the transition length. Strictly speaking, this series represents the arctangent transitions only in the limit where $\lambda \gg 4a$. We have found, however, that (18) gives a useful (if not exact) fit to the data even when this limit is not satisfied. This series underestimates the peak magnetization as the transitions are brought close together but has the property of eliminating the sharp junctions at $x = n\lambda / 4$, for n odd, which appear by directly matching arctangent transitions. We computed the fields by using (1), (2), (5), and (18), and then substituting them into (15) to obtain lineshape profiles. The lineshapes were then fit to the experimental data using a as an adjustable parameter. The resulting curves are shown as dashed lines in Fig. (5). We find that the best fit to the data corresponds to a transition of $a=0.7\mu$. The best fit was obtained at the longest wavelength, where this theory would be most applicable.

It should be emphasized that we attempted to fit the experimental data to numerous magnetization distributions, but the arctan distribution gave the best results. This is not surprising since the arctan distribution is the most widely accepted distribution seen in the literature. What actually happens, however, when the transitions are brought close together, might, according to our calculations, be somewhat surprising. It is commonly accepted that data density is limited by the increasing demagnetizing fields caused by the transitions being brought close together. Our calculations show, however, that the demagnetizing fields *decrease* as the transitions are brought close together. This is caused by the long tails of the arctan transitions which have the effect of drastically reducing the magnetization, and hence the demagnetizing fields, as the transitions are brought close together. It is this breakdown in the magnetization patterns that leads to the limits in data density. The usual arguments about increasing the coercivity to increase data density are still valid, because these arguments are made on the basis of isolated transitions. To increase data density you have to decrease the transition length. The transition length can only be decreased by increasing the coercivity, or the squareness of the hysteresis loop. Decreasing the magnetization, or the

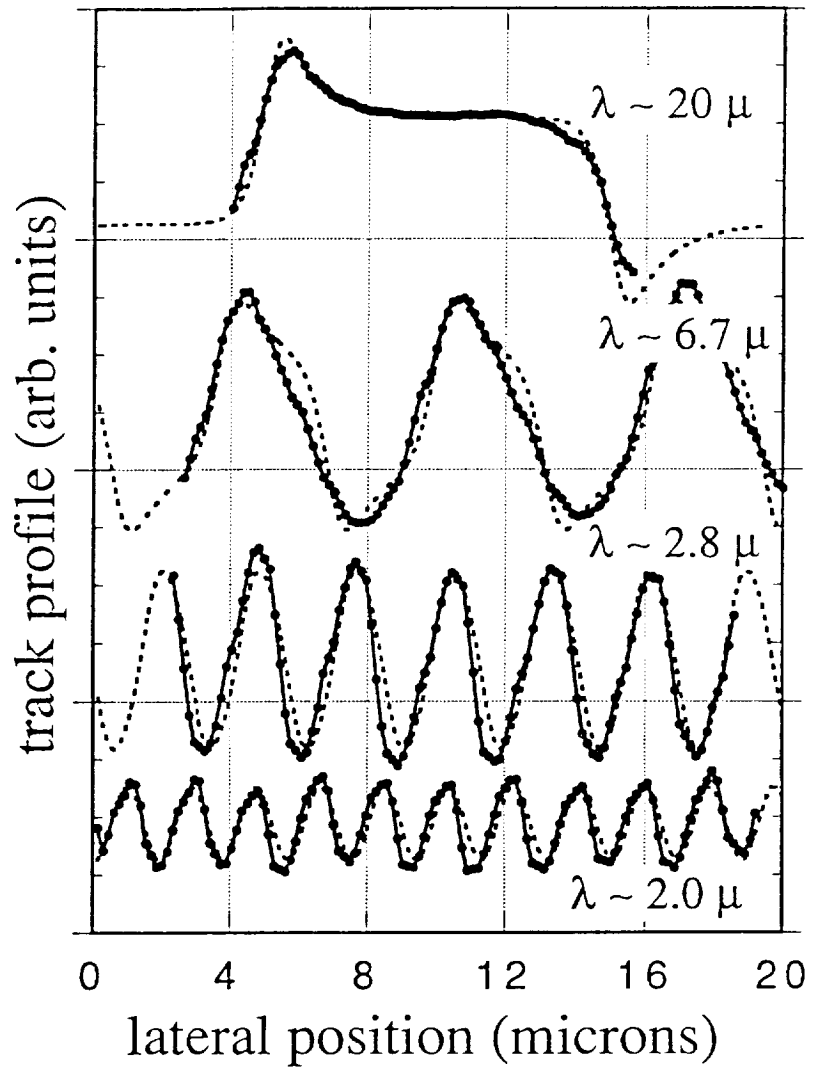
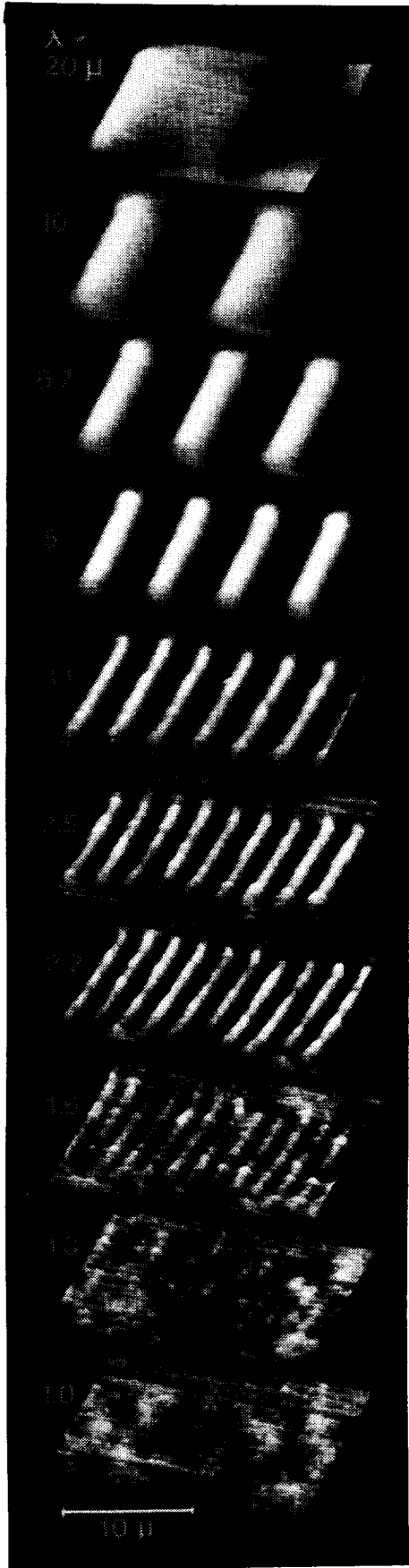


Figure 5. Solid curves: Average line profiles of representative images in Fig. 4; Dashed curves: calculated lineshapes for a constant transition length, $a = 0.7$ microns.

Figure 4. A series of MFSTM images of recorded patterns on thin-film media with progressively decreasing wavelengths.

media thickness, will also decrease the transition length but this will also decrease the readback signal. These conclusions are not new, but have been known for a long time [17], [18]. What is new is the actual observation of what is happening as the data density is increased. We have demonstrated that the magnetic force scanning tunneling microscope can be used as a powerful tool in studying these problems.

CONCLUSIONS

The MFSTM is shown to be a powerful technique for generating images of magnetization patterns. In particular, it has been used to yield images of persisting remanent data with minute details, and to investigate subtle features of overwritten data. We have demonstrated that the MFSTM is a powerful tool, useful in obtaining qualitative images and in deriving quantitative results. We used the technique in a study of data density and showed that the measured profiles could be adequately described by a model of arctan transitions. The best fit to the data gave a transition length of $a=0.7\mu$. Our theoretical analysis shows how the constituent magnetic fields from recorded magnetic patterns can be obtained from the images. We also show how the sensitivity of the microscope varies with the orientation of the probe, and how this relates to experimental data.

ACKNOWLEDGMENT

We are grateful to Mr. John Gorczyca and Dr. Mark Kryder at Carnegie Mellon University, Data Storage Systems Center for their cooperation and for providing recorded disks used in these experiments. Mr. Gorczyca and Dr. Kryder were also co-authors of two of our publications [4],[5].

REFERENCES

- [1] R. D. Gomez, E. R. Burke, A. A. Adly and I. D. Mayergoyz, "Magnetic Field Imaging by Using Magnetic Force Scanning Tunneling Microscopy," *Appl. Phys. Lett.* 60 (7), 17 February 1992 pp 906-908.
- [2] E. R. Burke, R. D. Gomez, A. A. Adly, and I. D. Mayergoyz, "Analysis of Tunneling Magnetic Force Microscopy Using a Flexible Triangular Probe," *IEEE Transactions on Magnetics* Vol. 28(5), September 1992 pp 3135-3137.
- [3] R. D. Gomez, E. R. Burke, A. A. Adly, and I. D. Mayergoyz, "Magnetic Force Scanning Tunneling Microscope Imaging of Overwritten Data," *IEEE Transactions on Magnetics* Vol. 28(5), September 1992 pp 3141-3143.
- [4] R. D. Gomez, E. R. Burke, A. A. Adly, I. D. Mayergoyz, J. A. Gorczyca and M. H. Kryder, "Magnetic Force Scanning Tunneling Microscopy of High Density Recording," Accepted for publication in the *Journal of Applied Physics*.
- [5] R. D. Gomez, E. R. Burke, A. A. Adly, I. D. Mayergoyz, J. A. Gorczyca and M. H. Kryder, "Microscopic Investigations of Overwritten Data," Accepted for publication in the *Journal of Applied Physics*.
- [6] I. D. Mayergoyz, A. A. Adly, R. D. Gomez, and E. R. Burke, "Experimental Testing of Point Charge Model of Magnetic Force Scanning Tunneling Microscopy," Accepted for publication in the *Journal of Applied Physics*.
- [7] I. D. Mayergoyz, A. A. Adly, R. D. Gomez, and E. R. Burke, "Magnetization Image Reconstruction from Magnetic Force Scanning Tunneling Microscopy Images," Accepted for publication in the *Journal of Applied Physics*.
- [8] P. Rice and J. Moreland, "Tunneling-stabilized Magnetic Force Microscopy of Bit Tracks on a Hard Disk," *IEEE Trans. Magn.*, vol. Mag-27, pp 3452-3454 (1991).
- [9] G. Binnig, H. Rohrer, Ch. Gerber, and E. Weibel, *Phys. Rev. Lett.* 49, 57 (1982).
- [10] A. Wadas, and P. Grutter, "Theoretical approach to magnetic force microscopy," *Phys. Rev. B*, vol. 39, no. 16, pp 12013-12017, June 1989.
- [11] A. Wadas, P. Grutter, and H.-J. Guntherolt, "Analysis of in-plane bit structure by magnetic force microscopy" *J. Appl. Phys.* 67 (7), pp 3462-3467 (1990).
- [12] R. L. Wallace, "The Reproduction of Magnetically Recorded Signals," *Bell Syst. Tech. J.*, vol. 30, p.1145, 1951.
- [13] D. Rugar, H. J. Mamin, P. Guethner, S. E. Lambert, J. E. Stern, I. McFadyen, and T. Yogi, "Magnetic force microscopy: General principles and application to longitudinal recording media" *J. Appl. Phys.* 68 (3), pp 1169-1183 (1990).
- [14] H. Edelman and M. Covault, "Design of Magnetic Recording Heads for High Track Densities," *IEEE Trans. Magn.*, vol 21, p 2583, 1985.
- [15] T. Yogi, C. Tsang, T. A. Nguyen, K. Ju, G. L. Gorman and G. Castillo, *IEEE Trans. Magn.* 26, 2271 (1990)
- [16] T. Lin, J. A. Christner, T. B. Mitchell, J-S. Gau, and P. K. Gorge, *IEEE Trans. Magn.* Vol. 25, 710 (1989).
- [17] R. I. Potter, "Analysis of saturation magnetic recording based on arctangent magnetization transitions," *J. Appl. Phys.*, vol. 41, no. 4, pp. 1647-1651, Mar. 1970.
- [18] M. L. Williams and R. L. Comstock, "An analytical model of the write process in digital magnetic recording." in *AIP Conf. Proc.* no. 5. pp. 738-742, 1971.